Superconducting ground state of quasi-one-dimensional K$_2$Cr$_3$As$_3$ investigated using μSR measurements

D. T. Adroja,[1,2,*] A. Bhattacharyya,[1,2,†] M. Telling,[1] Yu. Feng,[3] M. Smidman,[4] B. Pan,[3] J. Zhao,[3] A. D. Hillier,[1]
F. L. Pratt,[1] and A. M. Strydom[2]

[1]*ISIS Facility, Rutherford Appleton Laboratory, Chilton, Didcot Oxon OX11 0QX, United Kingdom*
[2]*Highly Correlated Matter Research Group, Physics Department, University of Johannesburg, P.O. Box 524,
Auckland Park 2006, South Africa*
[3]*State Key Laboratory of Surface Physics and Department of Physics, Fudan University, Shanghai 200433, China*
[4]*Center for Correlated Matter and Department of Physics, Zhejiang University, Hangzhou 310058, China*

The superconducting state of the newly discovered superconductor K$_2$Cr$_3$As$_3$, with a quasi-one-dimensional crystal structure ($T_c \sim 6$ K), is investigated using magnetization and muon-spin relaxation or rotation (μSR) measurements. Our analysis shows that the temperature dependence of the superfluid density obtained from transverse-field μSR measurements fits either to an isotropic s-wave character for the superconducting gap or to a d-wave model with line nodes. Furthermore, the goodness-of-fit (χ^2) values indicate that our data fit better to the d-wave model ($\chi^2 \sim 1$) than the s-wave model ($\chi^2 \sim 1.38$). Therefore our μSR analysis is more consistent with having line nodes than being fully gapped, which is in agreement with the results of the penetration depth measured using a tunnel diode oscillator technique. Our zero-field μSR measurements do reveal very weak evidence of the spontaneous appearance of an internal magnetic field below the transition temperature, which might indicate that the superconducting state is not conventional. This observation suggests that the electrons are paired via unconventional channels such as spin fluctuations, as proposed on the basis of theoretical models of K$_2$Cr$_3$As$_3$. Furthermore, from our transverse-field μSR study the magnetic penetration depth λ_L, superconducting carrier density n_s, and effective-mass enhancement m^* have been estimated to be $\lambda_L(0) = 432(4)$ nm, $n_s = 2.7 \times 10^{27}$ carriers/m^3, and $m^* = 1.75 m_e$, respectively.

PACS number(s): 74.70.Xa, 74.25.Op, 75.40.Cx

The superconducting gap structure of strongly correlated f- and d-electron superconductors is very important in understanding the physics of unconventional pairing mechanism in this class of materials. The recently discovered superconductors with a quasi-one-dimensional (Q1D) crystal structure, K$_2$Cr$_3$As$_3$ $T_c \sim 6.1$ K, Rb$_2$Cr$_3$As$_3$ $T_c \sim 4.8$ K, and Cs$_2$Cr$_3$As$_3$ $T_c \sim 2.2$ K, have been intensively investigated both experimentally and theoretically [1–7], as they are strong candidates for a multiband triplet pairing state. Searching for triplet superconductivity (SC) has been one of the major research efforts recently, partly due to its intrinsic connection to topologically related physics and quantum computations. These new superconductors are conjectured to possess an unconventional pairing mechanism [1,4–7]. There are several lines of experimental evidence. First, its upper critical field H_{c2} is significantly larger than the Pauli limit, indicating that the BCS-type pairing is unfavorable [2,8]. Second, strong electronic correlations, which are a common feature of unconventional SC, were revealed by the large electronic specific heat coefficient and non-Fermi-liquid transport behavior [1]. This is consistent with the the Q1D crystalline structure of A$_2$Cr$_3$As$_3$ (A = K, Rb, and Cs) and represents the possible realization of a Luttinger-liquid state [11]. Third, line nodal gap symmetry was revealed by London penetration depth measurements of K$_2$Cr$_3$As$_3$ [5].

Theoretically, by using density functional theory calculations, Wu *et al.* predicted K$_2$Cr$_3$As$_3$ to be near a novel

in-out coplanar magnetically ordered state and possess strong spin fluctuations [6,7]. Furthermore, it has been shown that a minimum three-band model based on the d_{z^2}, d_{xy}, and $d_{x^2-y^2}$ orbitals of one Cr sublattice can capture the band structure near the Fermi surfaces. In both weak- and strong-coupling limits, the standard random phase approximation and mean-field solutions consistently yield the triplet p_z-wave pairing as the leading pairing symmetry for physically realistic parameters [6,9,10]. The triplet pairing is driven by ferromagnetic fluctuations within the sublattice [6,7]. The gap function of the pairing state possesses line gap nodes on the $k_z = 0$ plane of the Fermi surface. So it is highly likely that electrons are paired via unconventional channels such as spin fluctuations in K$_2$Cr$_3$As$_3$. NMR measurements indeed reveal the enhancement of spin fluctuations towards T_c in K$_2$Cr$_3$As$_3$ [11]. Furthermore, Zhou *et al.* [12] have shown theoretically that at a small Hubbard U and moderate Hund's coupling, the pairing arises from the three-dimensional (3D) γ band and has $f_{y(3x^2-y^2)}$ symmetry, which gives line nodes in the gap function. At large U, a fully gapped p-wave state dominates in the Q1D α band.

A polycrystalline sample of K$_2$Cr$_3$As$_3$ was prepared as discussed in Ref. [1]. A high-quality powder sample of K$_2$Cr$_3$As$_3$ was characterized using neutron diffraction and magnetic susceptibility. The magnetization data were measured using a Quantum Design Superconducting Quantum Interference Device magnetometer. Muon spin relaxation/rotation (μSR) experiments were carried out on the MuSR spectrometer at the ISIS pulsed muon source of the Rutherford Appleton Laboratory, UK [13]. The μSR experiments were conducted in zero-field (ZF) and transverse-field (TF) mode. A

*devashibhai.adroja@stfc.ac.uk
†amitava.bhattacharyya@stfc.ac.uk

polycrystalline sample of $K_2Cr_3As_3$ was mounted in a sealed titanium (99.99%) sample holder under He-exchange gas, which was placed in a sorption cryostat that has a temperature range of 350 mK–50 K. It is to be noted that we used small pieces of the sample (not fine powder) to minimize the decomposition of the sample, as the sample is very air sensitive. Using an active compensation system the stray magnetic fields at the sample position were canceled to a level of 1 mG. TF-μSR experiments were performed in the superconducting mixed state in an applied field of 400 G, well above the lower critical field, $H_{c1} = 70$ G, of this material. Data were collected (a) in the field-cooled (FC) mode, where the magnetic field was applied above the superconducting transition and the sample was then cooled down to base temperature, and (b) in the ZF-cooled (ZFC) mode, where first the sample was cooled down to 2 K in ZF and then the magnetic field was applied. Muon spin relaxation is a dynamic method to resolve the type of pairing symmetry in superconductors [14]. The mixed or vortex state in the case of type II superconductors gives rise to a spatial distribution of local magnetic fields, which demonstrates itself in the μSR signal through a relaxation of the muon polarization. The asymmetry of the muon decay in ZF is calculated by $G_z(t) = [N_F(t) - \alpha N_B(t)]/[N_F(t) + \alpha N_B(t)]$, where $N_F(t)$ and $N_B(t)$ are the number of counts at the detectors in the forward and backward positions, respectively, and α is a constant determined from calibration measurements made in the paramagnetic state with a small (20-G) applied transverse magnetic field. Data were analyzed using the free software package WiMDA [15].

Analysis of the neutron powder diffraction at 300 K reveals that the sample is single phase and crystallizes with space group $P\bar{6}m2$ (No. 187). The hexagonal crystal structure obtained from neutron powder diffraction is shown in Fig. 1(a). The Q1D feature of $K_2Cr_3As_3$ is manifested by the chains of $[Cr_6(As_6)]_\infty$ octahedra running along the c direction. Magnetic susceptibility measurements show that SC occurs at 5.8 K and the superconducting volume fraction is close to 100% at 2 K [Fig. 1(b)], indicating the bulk nature of SC in $K_2Cr_3As_3$. The magnetization [$M(H)$] curve at 1.8 K [inset in Fig. 1(b)] shows a typical behavior for type II SC. In ZF, the temperature-dependent resistivity of $K_2Cr_3As_3$ is metallic [1,2]. Deviation from a linear temperature dependence is evident below 100 K and a T^3 dependence is roughly followed from just above T_c ($\sim$10 K) to $\sim$40 K [2]. At the superconducting transition, the specific heat jump is roughly 2.2 γT_c, which is larger than the simple s-wave BCS prediction 1.43 γT_c [1,2], possibly indicating strong coupling [16].

Figures 2(a) and 2(b) show the TF-μSR precession signals above and below T_c obtained in ZFC mode with an applied field of 400 G (well above $H_{c1} \sim 70$ Oe but below $H_{c2} \sim$ 320 kOe). Below T_c the signal decays with time due to the inhomogeneous field distribution of the flux-line lattice. The TF-μSR asymmetry spectra were fitted using an oscillatory decaying Gaussian function,

$$G_{z1}(t) = A_1 \cos(2\pi \nu_1 t + \phi_1) \exp\left(\frac{-\sigma^2 t^2}{2}\right)$$
$$+ A_2 \cos(2\pi \nu_2 t + \phi_2), \qquad (1)$$
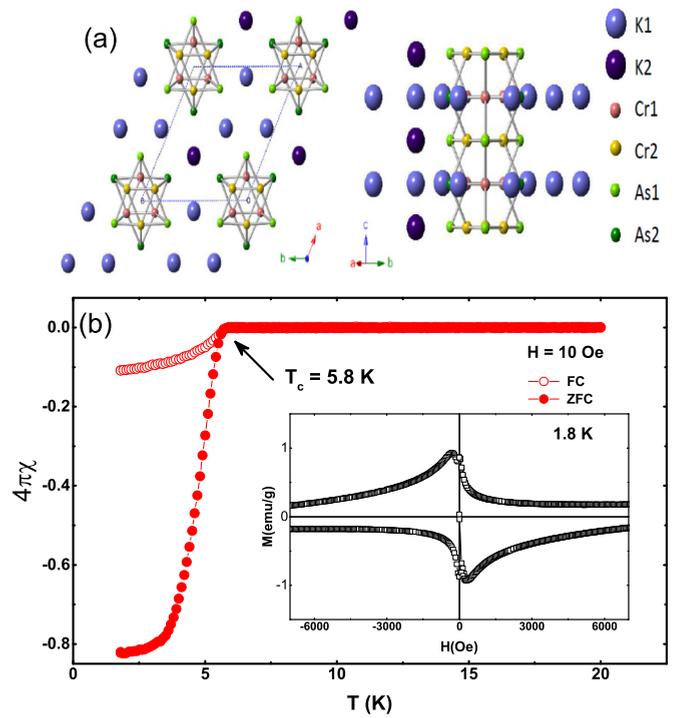
FIG. 1. (Color online) (a) Quasi-1D crystal structure of $K_2Cr_3As_3$ and (b) temperature dependence of the dc magnetic susceptibility measured in the zero-field–cooled (ZFC) and field-cooled (FC) states of $K_2Cr_3As_3$ in the presence of an applied magnetic field of 10 G. Inset: Magnetization vs field at 1.8 K.

where ν_1 and ν_2 are the frequencies of the muon precession signal from the sample and from the background signal from the Ti sample holder, respectively, and ϕ_i ($i = 1,2$) are the initial phase offsets. A_1 and A_2 are the muon initial asymmetries associated with the sample and background (from the Ti sample holder), respectively. The fits reveal the relative values of $A_1 = 25\%$ and $A_2 = 75\%$. It is noted that the value of A_2 is higher than that of A_1. The reason for this is that the muons have to first pass through the titanium foil (30 μm thick) and then stop in the sample. Another reason for the large background asymmetry is the fact that we have used small pieces of the sample rather than fine powder to minimize the decomposition of the sample, and hence it is possible that pieces might have settled down at the bottom of the sample holder when mounted vertically on the instrument. This also results in additional muons stopping directly in the titanium sample holder. In Eq. (1) the first term contains the total sample relaxation rate σ; there are contributions from both the vortex lattice (σ_{sc}) and nuclear dipole moments (σ_{nm}), which are assumed to be constant over the entire temperature range below T_c [where $\sigma = \sqrt{(\sigma_{sc}^2 + \sigma_{nm}^2)}$]. The contribution from the vortex lattice, σ_{sc}, was determined by quadratically subtracting the background nuclear dipolar relaxation rate obtained from the spectra measured above T_c. As σ_{sc} is directly related to the superfluid density, it can be modeled by [17]

$$\frac{\sigma_{sc}(T)}{\sigma_{sc}(0)} = 1 + 2\left\langle \int_{\Delta_k}^{\infty} \frac{\partial f}{\partial E} \frac{E dE}{\sqrt{E^2 - \Delta_k^2}} \right\rangle_{FS}, \qquad (2)$$
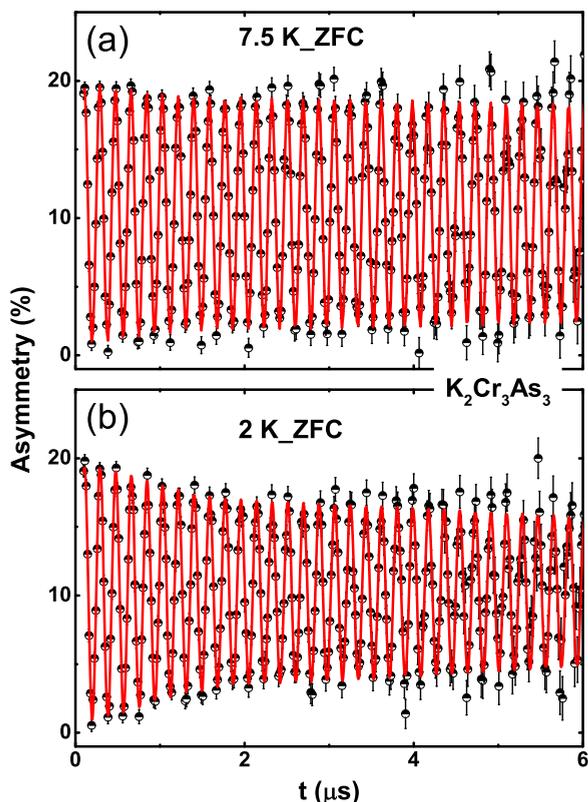
FIG. 2. (Color online) Transverse-field μSR time spectra (one component) for $K_2Cr_3As_3$ collected (a) at $T = 7.5$ K and (b) at $T = 2$ K in an applied magnetic field $H = 400$ G for the zero-field-cooled (ZFC) state.

FIG. 3. (Color online) (a) Temperature dependence of the muon depolarization rate $\sigma_{sc}(T)$ of $K_2Cr_3As_3$ collected in an applied magnetic field of 400 G in the zero-field-cooled (ZFC) and field-cooled (FC) modes. (b) $\sigma_{sc}(T)$ of the FC mode (symbols); lines are fits to the data using Eq. (2). The short-dashed (blue) line shows the fit using an isotropic single-gap s-wave model with $\Delta_0/k_B T_c = 1.6(1)$ and the solid (red) line and dotted (purple) lines show fits to the d-wave model with $\Delta_0/k_B T_c = 3.2(2)$ and $\Delta_0/k_B T_c = 2.40$, respectively. Inset: Plot of quality of fit χ^2 vs $\Delta_0/k_B T_c$.

where $f = [1 + \exp(-E/k_B T)]^{-1}$ is the Fermi function, and the angle brackets correspond to an average over the Fermi surface. The gap is given by $\Delta(T,\varphi) = \Delta_0 \delta(T/T_C) g(\varphi)$, φ is the azimuthal angle along the Fermi surface and the temperature dependence is given by $\delta(T/T_c) = \tanh[(\pi k_B T_c/\Delta_0)\sqrt{a(T_c/T - 1)}]$ [18], with $a = 1$ and $g(\varphi) = 1$ for the s-wave model [17] and $a = (2/3)(\Delta C/\gamma T_c)$ and $g(\varphi) = |\cos(2\varphi)|$, with $\Delta C/\gamma T_c = 2.2$, [2] for the d-wave model with line nodes.

Figure 3(a) shows the T dependence of σ_{sc}, measured in an applied field of 400 G through two modes: ZFC and FC. The temperature dependence of σ_{sc} shows the establishment of a flux-line lattice and indeed indicates a decrease in the magnetic penetration depth with decreasing temperature. Comparing the ZFC and FC data reveals a substantial difference. In the ZFC mode, σ_{sc} increases with decreasing temperature more rapidly than that in the FC mode and thus points to differences in the numbers of pinning sites and trapping energies, which are altered by magnetic fields and sample history. From the observed temperature dependence of σ_{sc}, the nature of the superconducting gap can be determined. The $\sigma_{sc}(T)$ data of $K_2Cr_3As_3$ can be well modeled by a single isotropic gap of 0.80(5) meV using Eq. (2) [see Fig. 3(b)]. This gives a value of $\Delta_0/k_B T_c = 1.6(1)$, which is slightly lower than the 1.764 expected for BCS superconductors. Considering that the tunnel diode study reveals the possibility of line nodes [5], we have also fitted σ_{sc} data using a d-wave model with line nodes. The fit to the nodal model [solid line in Fig. 3(b)] shows an

agreement similar to that of the s-wave fit [short-dashed line in Fig. 3(b)] but gives the higher value of $\Delta_0/k_B T_c = 3.2 \pm 0.2$. We also tried s-wave and d-wave fits with various fixed values of $\Delta_0/k_B T_c$ and allowing only $\sigma_{sc}(0)$ to vary, to compare the goodness-of-fit (χ^2) values between these two models [see inset in Fig. 3(b)]. The χ^2 values indicate that our data fit better to the d-wave model ($\chi^2 \sim 1$) than the s-wave model ($\chi^2 \sim 1.38$). Therefore our μSR analysis is more consistent with having line nodes than being fully gapped, which is in agreement with the results of the penetration depth measured using a tunnel diode oscillator technique [5].

Furthermore, the large value of $\Delta_0/k_B T_c = 3.2 \pm 0.2$ obtained from the d-wave fit indicates the presence of strong coupling, which is consistent with the value of a specific heat jump at the transition of $\Delta C/\gamma T_c = 2.2$, larger than the BCS value of 1.43. In addition, a ^{75}As NMR study of $K_2Cr_3As_3$ has

revealed the absence of the Hebel-Slichter coherence peak of $1/T_1$ just below T_c, which is followed by a steep decrease, in analogy with unconventional superconductors in higher dimensions with point or line nodes in the energy gap [11].

The Hebel-Slichter coherence peak of $1/T_1$ is a crucial test for the validity of the description of the superconducting state based on the conventional isotropic BCS *s*-wave model. The absence of the coherence peak in $1/T_1$ of $K_2Cr_3As_3$ suggests that an isotropic *s*-wave model is not an appropriate model to explain the gap symmetry. These NMR results of $K_2Cr_3As_3$ below T_c are similar to the case of unconventional superconductors, such as the high-T_c superconductor YBCO with *d*-wave pairing symmetry [19]. These results, along with our μSR analysis of $K_2Cr_3As_3$, suggest that the gap structure has line nodes.

The observed increase in σ_{sc} of $K_2Cr_3As_3$ gives rise to the high value of the muon spin depolarization rate below T_c and is related to the magnetic penetration depth. For a triangular lattice [14,21,22], $\frac{\sigma_{sc}(T)^2}{\gamma_\mu^2} = \frac{0.00371\phi_0^2}{\lambda^4(T)}$, where $\gamma_\mu/2\pi = 135.5$ MHz/T is the muon gyromagnetic ratio and $\phi_0 = 2.07 \times 10^{-15}$ T m^2 is the flux quantum. As with other phenomenological parameters characterizing a superconducting state, the penetration depth can also be related to microscopic quantities. Using London theory [20], $\lambda_L^2 = m^*c^2/4\pi n_s e^2$, where $m^* = (1 + \lambda_{e-ph})m_e$ is the effective mass and n_s is the density of superconducting carriers. Within this simple picture, λ_L is independent of the magnetic field. λ_{e-ph} is the electron-phonon coupling constant, which can be estimated from Θ_D and T_c using McMillan's relation [23], $\lambda_{e-ph} = \frac{1.04+\mu^* \ln(\Theta_D/1.45T_c)}{(1-0.62\mu^*)\ln(\Theta_D/1.45T_c)+1.04}$, where μ^* is the repulsive screened Coulomb parameter, usually assigned as $\mu^* = 0.13$. For $K_2Cr_3As_3$ we have $T_c = 5.8$ K and $\Theta_D = 216$ K, which, together with $\mu^* = 0.13$, we have estimated $\lambda_{e-ph} = 0.75$. $K_2Cr_3As_3$ is a type II superconductor, assuming that roughly all the normal-state carriers (n_e) contribute to the SC (i.e., $n_s \approx n_e$), hence we have estimated the magnetic penetration depth λ, superconducting carrier density n_s, and effective-mass enhancement m^* to be $\lambda_L(0) = 432(4)$ nm (from the *d*-wave fit), $n_s = 2.7 \times 10^{27}$ carriers/m^3, and $m^* = 1.75\ m_e$, respectively. More details of these calculations can be found in Refs. [24–26].

The time evolution of the ZF-μSR is shown in Fig. 4(a) for $T = 600$ mK and 8 K. In these relaxation experiments, any muons stopping on the titanium sample holder give a time-independent background. No signature of precession is visible, ruling out the presence of a sufficiently large internal magnetic field as seen in magnetically ordered compounds. One possibility is that the muon-spin relaxation is due to static, randomly oriented local fields associated with the nuclear moments at the muon site. The ZF-μSR data are well described by

$$G_{z2}(t) = A_1 e^{-\lambda t} + A_{bg}, \qquad (3)$$

where λ is the electronic relaxation rate, A_1 is the initial asymmetry, and A_{bg} is the background. The parameters A_1 and A_{bg} are found to be temperature independent. It is remarkable that λ shows a moderate increase [Fig. 4(b)] with an onset temperature of $\geqslant 6.0 \pm 0.1$ K, indicating the appearance of a spontaneous internal field or slowdown of spin fluctuations
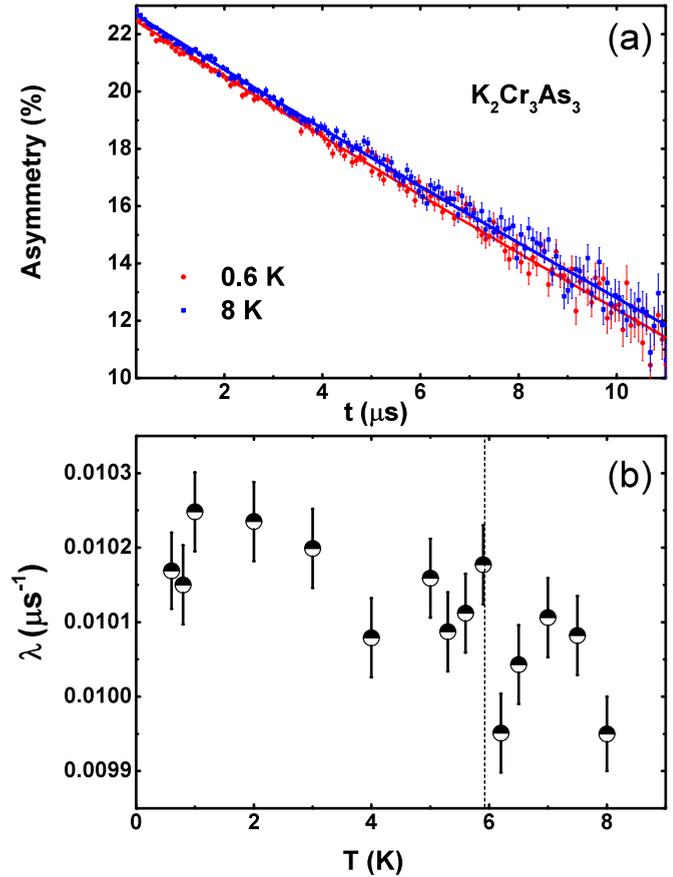
FIG. 4. (Color online) (a) Zero-field μSR time spectra for $K_2Cr_3As_3$ collected at 0.6 K [(red) circles] and 8.0 K [(blue) squares] are shown together with lines that are least squares fits to the data using Eq. (3). These spectra, collected below and above T_c, are representative of the data collected over a range of T. (b) Temperature dependence of the electronic relaxation rate of $K_2Cr_3As_3$ measured in zero magnetic field, where $T_c = 5.8$ K is shown by the dotted vertical line.

correlated with the SC. Based on this evidence, we propose that time reversal symmetry (TRS) might be broken in the SC state of $K_2Cr_3As_3$. Such a change in λ has only been observed in superconducting Sr_2RuO_4 [27], $LaNiC_2$ [28], $Lu_5Rh_6Sn_{18}$ [29], and $Y_5Rh_6Sn_{18}$ [30]. This increase in λ can be explained in terms of a signature of a coherent internal field with a very low frequency as discussed by Luke *et al.* [27] for Sr_2RuO_4. This suggests that the field distribution is Lorentzian in nature, similarly to Sr_2RuO_4, with an average of the second moment of the field distribution of 0.003 G in $K_2Cr_3As_3$, which is higher than the maximum field of 1 mG for the active ZF system on the MuSR spectrometer. This value is very small compared to the 0.5 G observed for Sr_2RuO_4 [27].

In summary, we have carried out ZF- and TF-μSR experiments in the superconducting state of $K_2Cr_3As_3$, which has a Q1D crystal structure. Our ZF μSR data reveal the presence of a very weak internal field (0.003 G) or slowdown of spin fluctuations in the superconducting state. From the TF-μSR we have determined the muon depolarization rate in ZFC and FC modes associated with the vortex lattice. The temperature dependence of σ_{sc} can be fitted to either a single-gap isotropic

s-wave or a d-wave model with line nodes. Further, the goodness-of-fit (χ^2) values indicate that our data fit better to the d-wave model than the s-wave model. Therefore our μSR analysis is more consistent with having line nodes than being fully gapped, which is in agreement with the results of the penetration depth measured using a tunnel diode oscillator technique. Considering the possible multiband nature of SC in $K_2Cr_3As_3$ one would expect more complex behavior of the gap function and hence the conclusions obtained from our TF-μSR study are in line with this. Further confirmation of the presence of line nodes in the superconducting gap requires μSR investigations of good-quality single crystals of $K_2Cr_3As_3$.

[1] J.-K. Bao, J.-Y. Liu, C.-W. Ma, Z.-H. Meng, Z.-T. Tang, Y.-L. Sun, H.-F. Zhai, H. Jiang, H. Bai, C.-M. Feng, Z.-A. Xu, and G.-H. Cao, Phys. Rev. X **5**, 011013 (2015).

[2] T. Kong, S. L. Budko, and P. C. Canfield, Phys. Rev. B **91**, 020507(R) (2015).

[3] Z.-T. Tang, J.-K. Bao, Z. Wang, H. Bai, H. Jiang, Y. Liu, H.-F. Zhai, C.-M. Feng, Z.-A. Xu, and G.-H. Cao, Sci. China Mater. **58**, 16 (2015).

[4] Z.-T. Tang, J.-K. Bao, Y. Liu, Y.-L. Sun, A. Ablimit, H.-F. Zhai, H. Jiang, C.-M. Feng, Z.-A. Xu, and G.-H. Cao, Phys. Rev. B **91**, 020506(R) (2015).

[5] G. M. Pang, M. Smidman, W. B. Jiang, J. K. Bao, Z. F. Weng, Y. F. Wang, L. Jiao, J. L. Zhang, G. H. Cao, and H. Q. Yuan, Phys. Rev. B **91**, 220502(R) (2015).

[6] X. Wu, C. Le, J. Yuan, H. Fan, and J. Hu, Chin. Phys. Lett. **32**, 057401 (2015).

[7] H. Zhong, X.-Y. Feng, H. Chen, and J. Dai, arXiv:1503.08965.

[8] F. F. Balakirev, T. Kong, M. Jaime, R. D. McDonald, C. H. Mielke, A. Gurevich, P. C. Canfield, and S. L. Bud'ko, Phys. Rev. B **91**, 220505(R) (2015)

[9] X. Wu, F. Yang, S. Qin, H. Fan, and J. Hu, arXiv:1507.07451v1.

[10] X. Wu, F. Yang, C. Le, H. Fan, and J. Hu, Phys. Rev. B **92**, 104511 (2015).

[11] H. Z. Zhi, T. Imai, F. L. Ning, J.-K. Bao, and G.-H. Cao, Phys. Rev. Lett. **114**, 147004 (2015).

[12] Y. Zhou, C. Cao, and F.-C. Zhang, arXiv:1502.03928v2.

[13] S. L. Lee, S. H. Kilcoyne, and R. Cywinski, *Muon Science: Muons in Physics, Chemistry and Materials* (SUSSP and IOP, Bristol, UK, 1999).

[14] J. E. Sonier, J. H. Brewer, and R. F. Kiefl, Rev. Mod. Phys. **72**, 769 (2000).

[15] F. L. Pratt, Physica B **289-290**, 710 (2000).

[16] J. P. Carbotte, Rev. Mod. Phys. **62**, 1027 (1990).

[17] R. Prozorov and R. W. Giannetta, Supercond. Sci. Technol. **19**, R41 (2006).

[18] F. Gross, B. S. Chandrasekhar, D. Einzel, K. Andres, P. J. Hirschfeld, and H. R. Ott, Z. Phys. B: Condens. Matter **64**, 175 (1986).

[19] T. Imai, T. Shimizu, H. Yasuoka, Y. Ueda, and K. Kosuge, J. Phys. Soc. Jpn. **57**, 2280 (1988).

[20] See, for example, N. W. Ashcroft and N. D. Mermin, *Solid State Physics* (Saunders College, Philadelphia, 1976), p. 738.

[21] See, for example, A. Amato, Rev. Mod. Phys. **69**, 1119 (1997).

[22] E. E. M. Chia, M. B. Salamon, H. Sugawara, and H. Sato, Phys. Rev. B **69**, 180509(R) (2004).

[23] W. McMillan, Phys. Rev. **167**, 331 (1968).

[24] A. D. Hillier and R. Cywinski, Appl. Magn. Reson. **13**, 95 (1997).

[25] V. K. Anand, D. Britz, A. Bhattacharyya, D. T. Adroja, A. D. Hillier, A. M. Strydom, W. Kockelmann, B. D. Rainford, and K. A. McEwen, Phys. Rev. B **90**, 014513 (2014).

[26] D. T. Adroja, A. D. Hillier, J.-G. Park, E. A. Goremychkin, K. A. McEwen, N. Takeda, R. Osborn, B. D. Rainford, and R. M. Ibberson, Phys. Rev. B **72**, 184503 (2005).

[27] G. M. Luke, Y. Fudamoto, K. M. Kojima, M. I. Larkin, J. Merrin, B. Nachumi, Y. J. Uemura, Y. Maeno, Z. Q. Mao, Y. Mori, H. Nakamura, and M. Sigrist, Nature (London) **394**, 558 (1998).

[28] A. D. Hillier, J. Quintanilla, and R. Cywinski, Phys. Rev. Lett. **102**, 117007 (2009).

[29] A. Bhattacharyya, D. T. Adroja, J. Quintanilla, A. D. Hillier, N. Kase, A. M. Strydom, and J. Akimitsu, Phys. Rev. B **91**, 060503(R) (2015).

[30] A. Bhattacharyya, D. T. Adroja, N. Kase, A. D. Hillier, J. Akimitsu, and A. M. Strydom, Sci. Rep. **5**, 12926 (2015).